Energies **2013**, *6*, 2949-2965; doi:10.3390/en6062949

OPEN ACCESS

energies

ISSN 1996-1073

www.mdpi.com/journal/energies

Article

Research on a Hierarchical Dynamic Automatic Voltage Control System Based on the Discrete Event-Driven Method

Wei Hu *, Le Zheng, Qiuyu Lu and Yong Min

State Key Lab of Power Systems, Department of Electrical Engineering, Tsinghua University, Beijing 100084, China; E-Mails: zhengl07@mails.tsinghua.edu.cn(L.Z.); luqiuyu22@126.com (Q.Y.L.); minyong@mail.tsinghua.edu.cn(Y.M.)

***** Author to whom correspondence should be addressed; E-Mail: huwei@mail.tsinghua.edu.cn; Tel.: +86-10-6279-4777; Fax: +86-10-6279-4698.

Received: 19 April 2013; in revised form: 23 May 2013 / Accepted: 30 May 2013 / Published: 17 June 2013

Abstract: In this paper, concepts and methods of hybrid control systems are adopted to establish a hierarchical dynamic automatic voltage control (HD-AVC) system, realizing the dynamic voltage stability of power grids. An HD-AVC system model consisting of three layers is built based on the hybrid control method and discrete event-driven mechanism. In the Top Layer, discrete events are designed to drive the corresponding control block so as to avoid solving complex multiple objective functions, the power system's characteristic matrix is formed and the minimum amplitude eigenvalue (MAE) is calculated through linearized differential-algebraic equations. MAE is applied to judge the system's voltage stability and security and construct discrete events. The Middle Layer is responsible for management and operation, which is also driven by discrete events. Control values of the control buses are calculated based on the characteristics of power systems and the sensitivity method. Then control values generate control strategies through the interface block. In the Bottom Layer, various control devices receive and implement the control commands from the Middle Layer. In this way, a closed-loop power system voltage control is achieved. Computer simulations verify the validity and accuracy of the HD-AVC system, and verify that the proposed HD-AVC system is more effective than normal voltage control methods.

Keywords: hierarchical control system; dynamic voltage control; hybrid control method; discrete event-driven; computer simulation

1. Introduction

With the ever-expanding scale and increasing complexity of power systems since 1960s–1970s, theories and technologies of automatic voltage control (AVC) aimed at secure, stable and economical operation of the whole power system have become important research subjects [1,2].

Currently, research on voltage control mostly focuses on power systems in a static status with stable operation, under the circumstances of which only slight voltage control adjustments are made so as to realize a certain function or certain indicators. In the existing secondary or tertiary-level voltage control [3–5], the time interval of control commands generated ranges from dozens of seconds to dozens of minutes, and even a couple of hours when the system is under stable operation, but in reality, the voltage fluctuates slowly and continuously due to external interference and the dynamic response time of system components. If the variation range and variation rate of the system voltage exceed the permitted limits, appropriate control measures are necessary to ensure the dynamic voltage quality and system security. This is referred to as dynamic voltage control. Despite the slow and lasting fluctuations of the voltage, methods used in research of static power system are no longer applicable. As dynamic components in the system (including generators, induction motor load, Var compensation equipment, *etc.*) all have a major impact on the system voltage, appropriate mathematical models of the power system components and dynamic methods are required to research dynamic voltage control.

To realize dynamic voltage stability control, concepts and methods of hybrid control system are introduced in this paper [6] to set up a hierarchical dynamic automatic voltage control (HD-AVC) system. A hybrid hierarchical control system model is set up, with the Top Layer analyzing the power system's dynamic voltage stability, constructing discrete events to drive the corresponding control block, and generating and sending out control strategies to the Middle Layer in case the system security is "threatened". Meanwhile, upon receiving control commands from the Top Layer, the Middle Layer conducts coordinated optimization control of multi-controllable components and sends control commands to the Bottom Layer. Control components of the Bottom Layer receive and execute the control commands from the Middle Layer. Finally in this paper an IEEE-22 bus system is adopted as an example for simulation research, verifying that the proposed system for dynamic voltage control is effective.

2. Model of HD-AVC System

Due to the longer control interval cycles of dynamic voltage control (ranging from tens of seconds to dozens of seconds), the relatively short electromagnetic dynamic process (usually less than one second) can be ignored when the dynamic behaviors of the system's internal components are considered. Therefore the system mathematical model is simplified, reducing the computing complexity and improving the analysis and control efficiency of the system. In a dynamic voltage hybrid control system, discrete event-driven and hierarchical control principles are adopted, with the control system structure [7] as seen in Figure 1.

Figure 1. HD-AVC system model.

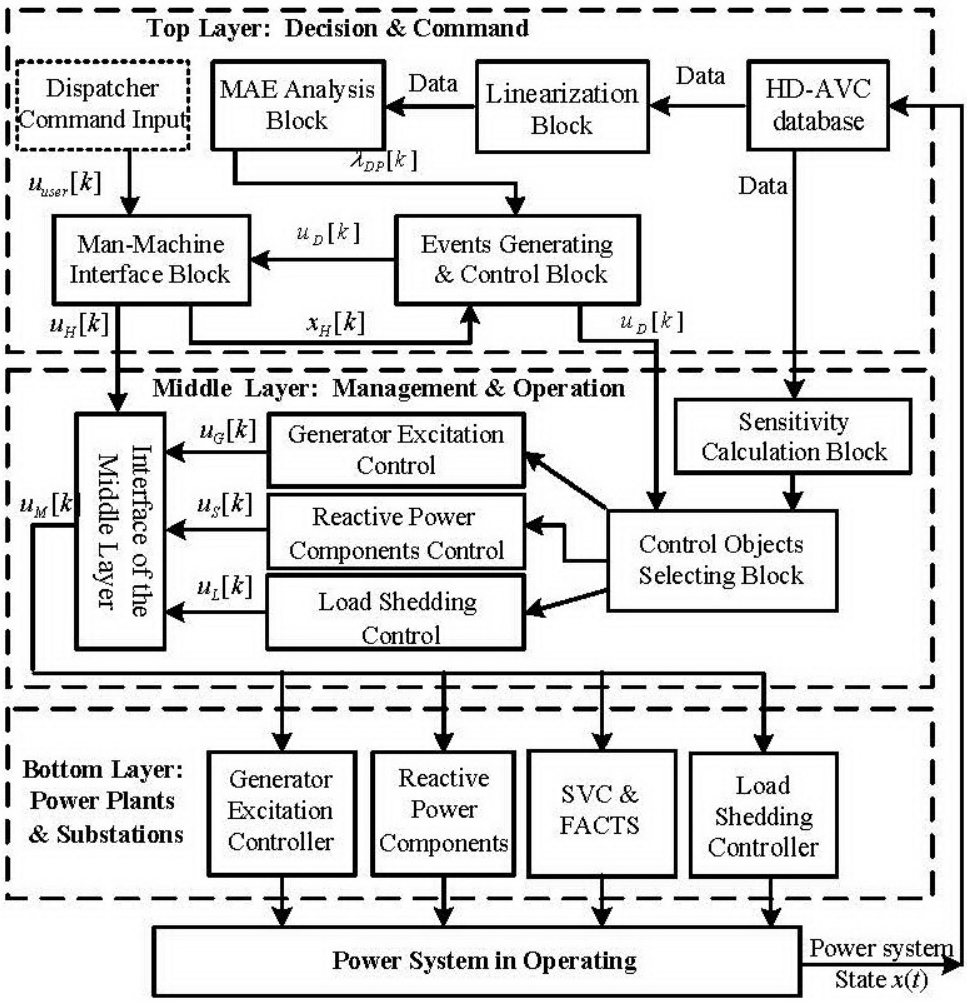

In the Top Layer of the HD-AVC system, a minimum amplitude eigenvalue (MAE) is used to analyze the power system's voltage security. Once any indicator exceeds the limit, discrete events are generated to drive the control blocks of the Top and Middle Layers. Driven by the discrete events, control blocks of the Top Layer generate optimal combinations of control solutions and send them to the Middle Layer. Through the interface the Middle Layer receives commands from the Top Layer, turns them into final control strategies and transmits the strategies to control equipment of the Bottom Layer. The controller of the Bottom Layer's control equipment makes adjustments according to the control strategies received, changing the system's operational status to improve the dynamic voltage quality as well as system security and stability. The various control layers of the HD-AVC system are explained in detail in the following sections.

3. The Top Layer of Decision and Command

The primary target of the Top Layer is to ensure voltage security and stability in the power system as well as to improve the dynamic quality of voltage. In the Top Layer, discrete events are constructed to drive the control. Meanwhile, coordination among various voltage control components is taken into consideration in this layer.

3.1. Dynamic Voltage Stability Analysis Method

When analyzing the system dynamic voltage security and stability, the control interval is relatively longer with the system status changing slowly. Therefore linearized differential-algebraic-equations (DAE) are used to describe the power system's dynamics. Through analyzing the eigenvalue of the relevant DAE system, judgment is made regarding the stability of the power system.

Since the dynamic performance of generators and induction motors in power system are described by differential equations f(x,y,u) and the power grid is supposed to meeting the constraints of power flow algebraic equations g(x,y,u), the power system can be described by differential-algebraic-equations [8,9] as follows:

$$\begin{cases} \dot{\mathbf{x}}(t) = \mathbf{f}(\mathbf{x}(t), \mathbf{y}(t), \mathbf{u}) \\ \mathbf{0} = \mathbf{g}(\mathbf{x}(t), \mathbf{y}(t), \mathbf{u}) \end{cases} \tag{1}$$

where x denotes the dynamic variables such as rotor angel and angular velocity of generators; y denotes the algebraic variables like voltage and angle of each bus in power system; and u denotes the controlling variables like generator excitation output in this paper. By linearizing the above system in expression Equation (1) at the operating point, we get the following equation:

$$[\Delta\dot{\mathbf{x}}] = \mathbf{J} \cdot [\Delta\mathbf{x}] + \mathbf{B} \cdot [\Delta\mathbf{y}] + \mathbf{C} \cdot [\Delta\mathbf{u}] \tag{2}$$

where J, B and C can be referred to as in literature [7].

Through linearization, we have acquired the linear differential equations in Equation (2) which describe the dynamic process of the power system. Based on the linear differential equations, we can analyze the stability of the system through the eigenvalues of the coefficient matrix. The most common solution for an eigenvalue is the QR method [8], but the matrix dimension limits the application of conventional QR methods. Generally speaking, conventional QR methods can only help acquire eigenvalues of matrixes of less than 200 ranks. However, in reality hundreds of generators and loads run in large-scale power systems, therefore QR methods are no longer applicable, and order reduction of the original system needs to be accomplished before the iteration method can be applied [8].

3.2. Analysis of Minimum Amplitude Eigenvalue

As the minimum amplitude eigenvalue (MAE) is acquired through the above steps, the stability status of the power system can be judged by MAE's amplitude, and the discrete variables are formed and sent to the discrete control blocks. Furthermore we define the following mapping:

$$\mathbf{T}_R: \quad \lambda_{\min}[k] \to \lambda_{DP}[k] \tag{3}$$

where $\lambda_{\min}[k]$ denotes the MAE calculated at the end of the k-th control interval; $\lambda_{DP}[k]$ denotes the discrete variable, as well as the input of the subsequent discrete control. $\lambda_{DP}[k]$ is valued by the following rules:

$$\lambda_{DP}[k] = \begin{cases} 1 & \text{if} \quad \|\lambda_{\min}[k]\| > \lambda_{safe} \\ 0 & \text{if} \quad \lambda_{safe} \geq \|\lambda_{\min}[k]\| > \lambda_{alert} \\ -1 & \text{if} \quad \lambda_{alert} \geq \|\lambda_{\min}[k]\| \end{cases} \tag{4}$$

where λ_{safe} denotes the pre-set minimum security value; λ_{alert} denotes the pre-set alert value.

In addition to using the MAE index, we can also use other kinds of voltage stability indexes, which can be easily improved for use in the proposed HD-AVC system.

3.3. Events and Control for Voltage Stability

As the amplitude of MAE, $\lambda_{\min}[k]$ is acquired. It is sent together with the status-discrete value of pilot buses [7] to the discrete control blocks and form discrete events. Thus we can come to the control output.

The input-output characteristics of the discrete control block are defined as follows:

$$\begin{cases} x_{DE}[k] = E_{DE}(x_{DP}[k], \lambda_{DP}[k]) \\ u_D[k] = O_{DE}(x_{DE}[k], x_H[k]) \end{cases} \tag{5}$$

where the parameter k stands for after k control intervals; E_{DE} and O_{DE} refer to status transmitting function and output function of the discrete control block respectively; $x_{DE}[k]$ and $u_D[k]$ denote status variables and output events of the control block respectively; $x_{DP}[k]$ refers to the status discrete magnitude; $x_H[k]$ is the output of the Top Layer at interval $(k-1)$, as following:

$$x_H[k] = u_H[k-1] \tag{6}$$

As shown in Equation (5), the status transmitting function E_{DE} transforms the discrete magnitude representing system security and stability together with the discrete magnitude representing status of the pilot buses into discrete events, and the discrete events drive the output of discrete control. Three "events" are defined as follows:

$$x_{DE}[k] \in \{P_{imp}, P_{acc}, P_{bad}\} \tag{7}$$

where P_{imp}, P_{acc} and P_{bad} stand for sound, ordinary and poor quality of voltage control. In order to get the status transmitting function E_{DE}, the temporary variables $x_{vol}[k]$, $x_{dec}[k]$ and $x_{inc}[k]$ are defined as follows:

$$\begin{cases} X_{vol}[k] = \{x_{vol}[k] \mid x_{vol}[k] = \sum_{i=1}^{\alpha_P} x_{1i}[k]\} \\ X_{dec}[k] = \{x_{dec}[k] \mid x_{dec}[k] = \sum_{i=1}^{\alpha_P} x_{2i}[k]\} \\ X_{inc}[k] = \{x_{inc}[k] \mid x_{inc}[k] = \sum_{i=1}^{\alpha_P} x_{3i}[k]\} \end{cases} \tag{8}$$

where α_P refers to the number of pilot buses, and: $x_{1i}[k] = \{1, 0, -1\}$ voltage status of pilot buses i; $x_{2i}[k] = \{1, 0, -1\}$ voltage decrease speed rate status of pilot buses i; $x_{3i}[k] = \{1, 0, -1\}$ voltage increase speed rate status of pilot buses i.

For the above variables, a value of 1, 0, −1 means the corresponding plant status is acceptable, inadequate or undesirable, respectively. The criteria of the acceptable, inadequate and undesirable statuses are decided by the designer, and with the different power systems, the criteria are different. In this paper, the three statuses are defined as follows:

$$x_{1i}[k] = \begin{cases} 1 & \text{if } \left\| x_{Pi}[k] - x_{Pi}^{s\tan} \right\| < \varepsilon_{1i} \\ 0 & \text{if } \varepsilon_{1i} \le \left\| x_{Pi}[k] - x_{Pi}^{s\tan} \right\| < \varepsilon_{2i} \\ -1 & \text{if } \varepsilon_{2i} \le \left\| x_{Pi}[k] - x_{Pi}^{s\tan} \right\| \end{cases} \tag{9}$$

$$x_{2i}[k]=\begin{cases}1 & \text{if } (0\le x_{Pi}[k-1]-x_{Pi}[k]<\varepsilon_{3i})\bigcup(0<x_{Pi}[k]-x_{Pi}[k-1]<\varepsilon_{5i})\\ 0 & \text{if } (\varepsilon_{3i}\le(x_{Pi}[k-1]-x_{Pi}[k]<\varepsilon_{4i})\bigcup(x_{Pi}[k]-x_{Pi}[k-1]\ge\varepsilon_{5i})\\ -1 & \text{if else}\end{cases} \tag{10}$$

$$x_{3i}[k]=\begin{cases}1 & \text{if } (0\le x_{Pi}[k]-x_{Pi}[k-1]<\varepsilon_{5i})\bigcup(0<x_{Pi}[k-1]-x_{Pi}[k]<\varepsilon_{3i})\\ 0 & \text{if } (\varepsilon_{6i}\le x_{Pi}[k]-x_{Pi}[k-1]<\varepsilon_{5i})\bigcup(x_{Pi}[k]-x_{Pi}[k-1]\ge\varepsilon_{3i})\\ -1 & \text{if else}\end{cases} \tag{11}$$

where $\varepsilon_{ji}(j=1,\ \cdots,\ 6)$ are the setting boundary values of pilot bus i, $x_{Pi}^{s\tan}$ is the setting ideal voltage value of pilot bus i. The above boundary values and the voltage value are not set by unified and fixed rules, and they can be set differently according to the specific circumstances in power system. Finally, the logic rules to form discrete "events" are defined as follows:

$$x_{DE}[k]=\begin{cases}P_{imp} & \begin{cases}\text{if } (\lambda_{DP}[k]=1)\\ \text{if } (\lambda_{DP}[k]=0)\bigcap(x_{vol}[k]>x_{vol}[k-1])\\ \text{if } (\lambda_{DP}[k]=0)\bigcap(x_{vol}[k]=M)\end{cases}\\ P_{acc} & \begin{cases}\text{if } (\lambda_{DP}[k]=0)\bigcap((x_{vol}[k]=x_{vol}[k-1]\ne M)\\ \quad\bigcap\overline{((x_{dec}[k]\le x_{dec}[k-1])\bigcap(x_{inc}[k]\le x_{inc}[k-1]))}\ )\end{cases}\\ P_{bad} & \begin{cases}\text{if } (\lambda_{DP}[k]=\text{-}1)\\ \text{if } (\lambda_{DP}[k]=0)\bigcap(x_{vol}[k]<x_{vol}[k-1])\\ \text{if } (\lambda_{DP}[k]=0)\bigcap((x_{vol}[k]=x_{vol}[k-1]\ne M)\\ \quad\bigcap(x_{dec}[k]\le x_{dec}[k-1])\ \bigcap(x_{inc}[k]\le x_{inc}[k-1]))\end{cases}\end{cases} \tag{12}$$

The logic rules of the above discrete events are not fixed, and can be modified according to the system's specific conditions.

The output function $O_{DE}(\cdot)$ in Equation (5) is shown in Figure 2, where the arrow indicates that due to the emergence of discrete events $x_{DE}[k]$, the control output shifts from that in the last interval $x_H[k]$ to the present interval $u_D[k]$. As defined below:

$$u_D[k]\in\{0,\ 1,\ 2,\ 3,\ 4,\ 5,\ 6,\ 7\} \tag{13}$$

The implication of the numbers in Equation (10) is shown in Figure 2. As an illustration, Figure 2 shows that no path is available to convert from 2 to 0, from 3 to 0, from 6 to 3, from 7 to 5 and from 7 to 6. This is designed so as to minimize the system operation cost, prolong service lifetime of reactive compensation equipment and minimize users' losses. Among power system's control measures, generator regulation is given top priority, followed by reactive power compensation control, while load-shedding is the last choice.

Figure 2. Discrete output function in the top layer.

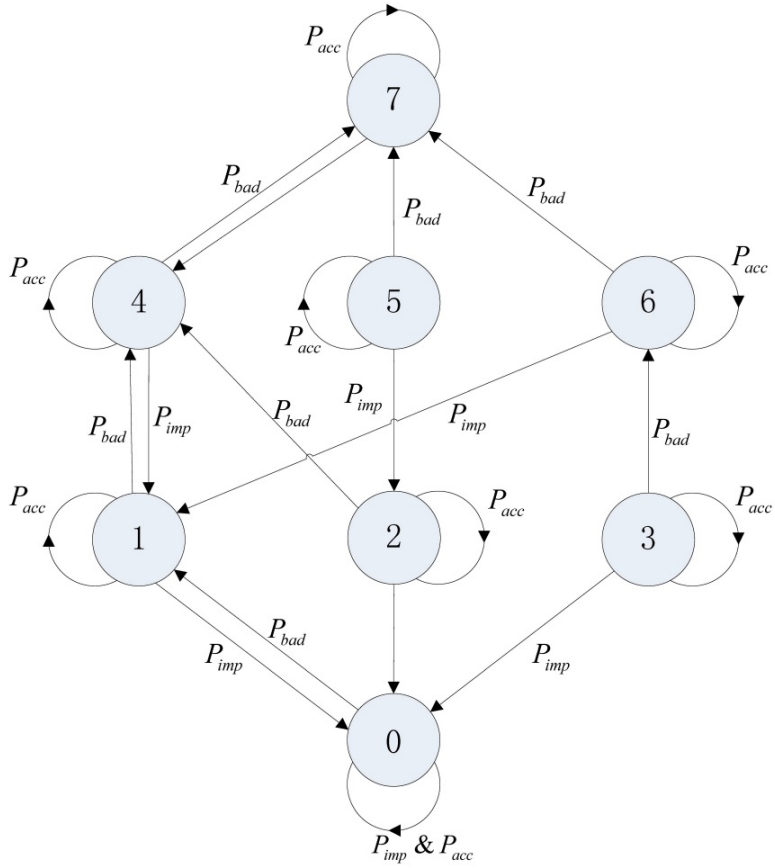

3.4. Man-Machine Interface Block

After the discrete control block, we defined a Man-Machine Interface Block, which can accept the system dispatchers' control commands. The supreme authority is given to the dispatchers' control commands in the interface block. By the following mapping T_u, we can get the Top Layer's control output:

$$T_u : x_u[k] \to u_H[k] \tag{14}$$

where $x_u[k] = [u_{user}[k],\ u_D[k]]^T$ and $u_{user}[k] \in \{0,\ 1,\ 2,\ 3,\ 4,\ 5,\ 6,\ 7,\ 8\}$. The values of 0 to 7 have the same meaning of $u_D[k]$, and 8 represents that theydo not have any dispatcher control command input. We define the output of Man-Machine Interface Block as below:

$$u_H[k] = \begin{cases} u_D[k] & \text{if}(u_{user}[k] = 8) \\ u_{user}[k] & \text{if}(u_{user}[k] \neq 8) \end{cases} \tag{15}$$

where $u_H[k] \in \{0,\ 1,\ 2,\ 3,\ 4,\ 5,\ 6,\ 7\}$, and the values of 0 to 7 have the same meaning of $u_D[k]$.

4. The Middle Layer of Management and Operation

The Middle Layer is set to receive control commands from the Top Layer, coordinating multi-control objects and optimizing multi-objectives, and making coordinated and optimal control strategies sent to control devices of the Bottom Layer.

4.1. Sensitivity Calculation

More control objects exist in the middle layer, including the reference voltage of generator excitation, the reactive compensation equipment and the quantity of under-voltage load-shedding, *etc.* As research results indicate a significant linear relationship between the power system's voltage stability margin and the parameters of the control objects near the operating point [10], MAE sensitivity of the control parameters can be applied to acquire the control variable values. According to the literature [8], MAE sensitivity of parameter α is as follows:

$$\frac{\partial \lambda_{\min}}{\partial \alpha} = \frac{\mathbf{v}_{L\min}^{T} \cdot \left[\frac{\partial \mathbf{J}}{\partial \alpha}\right] \cdot \mathbf{v}_{R\min}}{\mathbf{v}_{L\min}^{T} \cdot \mathbf{v}_{R\min}} \tag{16}$$

Thus within interval k, the sensitivity of minimum amplitude eigenvalue $\lambda_{\min}[k]$ related to the control variables is [7]:

$$\frac{\partial \lambda_{\min}[k]}{\partial u} = \frac{\mathbf{v}_{rL}^{T} \cdot \frac{\partial \mathbf{J}_r(\lambda_{\min}[k],\ u)}{\partial u} \cdot \mathbf{v}_{rR}}{\mathbf{v}_{rL}^{T} \cdot (\mathbf{I} - \frac{\partial \mathbf{J}_r(\lambda_{\min}[k],\ u)}{\partial \lambda_{\min}[k]}) \cdot \mathbf{v}_{rR}} \tag{17}$$

where $\mathbf{J}_r(\lambda_{\min}[k],\ u)$ denotes the characteristic coefficient matrix, and $\mathbf{v}_{rL}$ and $\mathbf{v}_{rR}$ stand for the left and right eigenvectors corresponding to the minimum amplitude eigenvalue $\lambda_{\min}[k]$, respectively. The control variable **u** includes the pre-set value of generator excitation voltage E'_G, the voltage control V_S of the bus with reactive compensation equipment and the load-shedding control (*i.e.*, to change the initial value P_{D0} and Q_{D0}).

4.2. Control Strategy-Making

The control variable of generator buses, the reactive compensate buses and the load-shedding buses are acquired respectively in this step.

4.2.1. Control of Generator Excitation Voltage Pre-Set Value

In order to have the MAE's amplitude $\|\lambda_{\min}[k]\|$ reach the pre-set minimum security value λ_{safe}, by making use of the sensitivity relationship we define optimization issues as following (supposing there are α_G generator buses in the system):

$$\min z = \left\{ \left| k_G (d_{safe} - \|\lambda_{\min}[k]\|) - \sum_{i=1}^{\alpha_G} \left(\frac{\partial \lambda_{\min}[k]}{\partial E'_{Gi}}\right) \cdot \Delta E'_{Gi}[k] \right| \right\} + \sum_{i=1}^{\alpha_G} w_{Gi} \left| \Delta E'_{Gi}[k] \right| \tag{18}$$

where $\Delta E'_{Gi}[k]$ indicates the voltage change value of generator i within interval k, while k_G and w_{Gi} refer to pre-set weight coefficients. Moreover, each generator bus is supposed to satisfy the constraints

as follows:

$$\begin{cases} E'^{MIN}_{Gi} \le E'_{Gi}[k] + \Delta E'_{Gi}[k] \le E'^{MAX}_{Gi} \\ \left|\Delta E'_{Gi}[k]\right| \le \Delta E'^{MAX}_{Gi} \end{cases} \quad i = 1, \cdots, \alpha_G \tag{19}$$

where E'^{MIN}_{Gi} and E'^{MAX}_{Gi} represent the allowed minimum and maximum voltage value of generator i, and $\Delta E'^{MAX}_{Gi}$ denotes the maximum allowed change value in voltage control. The first term in Equation (19) ensures that the generator voltage ranges within limits, and the second term ensures that the excitation voltage change value is not significant enough to make the system oscillate. By solving Equations (18) and (19), we can acquire the change value of given voltage $\Delta E'_{Gi}[k]$ of excitation at each generator bus.

4.2.2. Control of Pre-Set Voltage Value of Reactive Power Compensator

Similar to generator voltage control, to have the MAE's amplitude $\left\|\lambda_{\min}[k]\right\|$ reach the pre-set minimum security value λ_{safe}, by making use of the sensitivity relationship we define optimization issues as follows (supposing there are α_S reactive power compensator buses in the system):

$$\min z = \left\{ \left| k_S (d_{safe} - \left\|\lambda_{\min}[k]\right\|) - \sum_{i=1}^{\alpha_S} \left(\frac{\partial \lambda_{\min}[k]}{\partial V_{Si}}\right) \cdot \Delta V_{Si}[k] \right| \right\} + \sum_{i=1}^{\alpha_S} w_{Si} \left|\Delta V_{Si}[k]\right| \tag{20}$$

where $\Delta V_{Si}[k]$ indicates the voltage change value of reactive power compensator i within interval k; while k_S and w_{Si} are defined as pre-set weight coefficients. Moreover, each reactive power compensator bus is supposed to satisfying the constraints as follows:

$$\begin{cases} V^{MIN}_{Si} \le V_{Si}[k] + \Delta V_{Si}[k] \le V^{MAX}_{Si} \\ \left|\Delta V_{Si}[k]\right| \le \Delta V^{MAX}_{Si} \end{cases} \quad i = 1, \cdots, \alpha_S \tag{21}$$

where V^{MIN}_{Si} and V^{MAX}_{Si} represent the minimum and maximum allowed voltage value of reactive power compensator i; and ΔV^{MAX}_{Si} refers to the maximum allowed change value in voltage control. The first term in Equation (21) ensures that the reactive power compensator voltage value changes within limits, and the second term ensures that the change value of the bus voltage is not significant enough to make the system oscillate. By solving Equations (20) and (21), we can get the given voltage value of each reactive power compensator bus.

4.2.3. Volume Control of Load-Shedding at Load-Shedding Buses

Similarly, in order to have the MAE's amplitude $\left\|\lambda_{\min}[k]\right\|$ reach the pre-set minimum security value λ_{safe}, by making use of the sensitivity relationship we define optimization issues as follows (supposing there are α_L load-shedding buses in the system):

$$\min z = \left\{ \left| k_L (d_{safe} - \left\|\lambda_{\min}[k]\right\|) - \sum_{i=1}^{\alpha_L} \left(\frac{\partial \lambda_{\min}[k]}{\partial P_{Li}}\right) \cdot \Delta P_{Li}[k] \right| \right\} + \sum_{i=1}^{\alpha_L} w_{Li} \left|\Delta P_{Li}[k]\right| \tag{22}$$

where $\Delta P_{Li}[k]$ indicates the value change of active load at load-shedding bus i within interval k; while k_L and w_{Li} refer to pre-set weight coefficients. Moreover, each load-shedding bus is supposed to satisfying the constraints as follows:

$$\begin{cases} \max\{P_{Li}^{MIN}; Q_{Li}^{MIN} / tg\varphi_{Li}\} \le P_{Li}[k] - \Delta P_{Li}[k] \\ \sum_{i \in \alpha_L} \Delta P_{Li}[k] \le \Delta P_L^{MAX} \end{cases} \quad i = 1, \cdots, \alpha_L \tag{23}$$

where φ_{Li} indicates the power factor angle of bus i; while P_{Li}^{MIN} and Q_{Li}^{MIN} represent the minimum active and reactive power of bus i; and ΔP_L^{MAX} stands for the maximum allowed value change in load-shedding control. The first term in Equation (23) defines the minimum load of each load-shedding bus, and the second term ensures that the value change of the active power is not significant enough to make the system oscillate. By solving Equations (22) and (23), we can get the given excitation voltage value of each bus.

4.3. Interface of the Middle Layer

The interface of the Middle Layer receives control commands from the Top Layer, selects the most appropriate control method among various alternatives, and sends coordinated optimization instructions to the control equipment of the Bottom Layer. The mapping is defined as follows:

$$\mathbf{u}_M(t) = \mathbf{T}_{\text{inter}}(\mathbf{u}_G[k], \mathbf{u}_S[k], \mathbf{u}_L[k], u_H[k]) \tag{24}$$

where $\mathbf{u}_M(t)$ represents the output instructions of hybrid control, constantly being sent out within interval k till the next command is given. In the mapping above, $\mathbf{u}_G[k], \mathbf{u}_S[k], \mathbf{u}_L[k]$ denote the generator bus control vector, the reactive power compensation bus control vector, and the load-shedding bus control vector, respectively, all within interval k. $\mathbf{u}_H[k]$ refers to the instruction from the Top Layer within interval k. The input and output logic is defined as follows:

$$u_M(t) = \begin{cases} 0 & \text{if}(u_H[k] = 0) \\ \mathbf{u}_G[k] & \text{if}(u_H[k] = 1) \\ \mathbf{u}_S[k] & \text{if}(u_H[k] = 2) \\ \mathbf{u}_L[k] & \text{if}(u_H[k] = 3) \\ \mathbf{u}_G[k] \,\&\, \mathbf{u}_S[k] & \text{if}(u_H[k] = 4) \\ \mathbf{u}_S[k] \,\&\, \mathbf{u}_L[k] & \text{if}(u_H[k] = 5) \\ \mathbf{u}_G[k] \,\&\, \mathbf{u}_L[k] & \text{if}(u_H[k] = 6) \\ \mathbf{u}_G[k] \,\&\, \mathbf{u}_S[k] \,\&\, \mathbf{u}_L[k] & \text{if}(u_H[k] = 7) \end{cases} \tag{25}$$

By taking the above steps, we have acquired the hybrid automatic dynamic voltage control instructions, which are to be executed by the control equipment of the Bottom Layer and thus ensure system security and stability. Meanwhile, the validity of hybrid control is verified by computer simulation, as explained in the following paragraphs.

5. The Bottom Layer

Calculation results including control vectors of the generator bus, the reactive power compensation bus and the load-shedding bus of the Middle Layer are delivered to the control equipment of the Bottom Layer for execution. In the Bottom Layer, the MAE's amplitude of voltage stability mode is enabled to reach the pre-set voltage value of the Top Layer, ensuring system voltage security. Closed-loop control of dynamic voltage is realized in the Bottom Layer, thus eliminating discrete events in the Top Layer and ensuring system security.

6. Simulation Results

Computer simulations have verified the validity of hybrid dynamic voltage control as proposed. The simulation is made through Power System Analysis Software Package (PSASP), developed by China Electric Power Research Institute (CEPRI, Beijing, China).

6.1. Simulation in IEEE 22-Bus System

The IEEE 22-bus system is shown as in Figure 3, where the parameters of the power system, generators and transformers are introduced in reference [7]. A model of constant impedance (60%) combined with induction load motor (40%) is adopted. In the simulation, the reactive load in each load bus is evenly doubled from second 0 to second 60. Under such circumstances the three following programs are studied by comparison: ① traditional AVR control applied to all the generators; ② traditional secondary voltage control applied to all the generators; ③ hierarchical control applied to all the generators, with certain load-shedding and reactive power devices taken into consideration at the same time. The control interval is defined as 10 seconds.

Figures 4 and 5 show the voltage curve of key bus No.11 and No.16 in the three control programs mentioned, respectively. Figures 6–8 show the voltage, output active power and reactive power curve of generator bus No.2. The above figures indicate that the system starts voltage collapse in about 50 seconds when traditional AVR control is applied. The situation is improved when traditional secondary voltage control is applied, with the system starting voltage collapse in about 70 s. However, with the proposed dynamic hybrid automatic voltage control, the system is under effective control, with system security enabled and voltage collapse avoided.

Figure 3. IEEE 22-bus system.

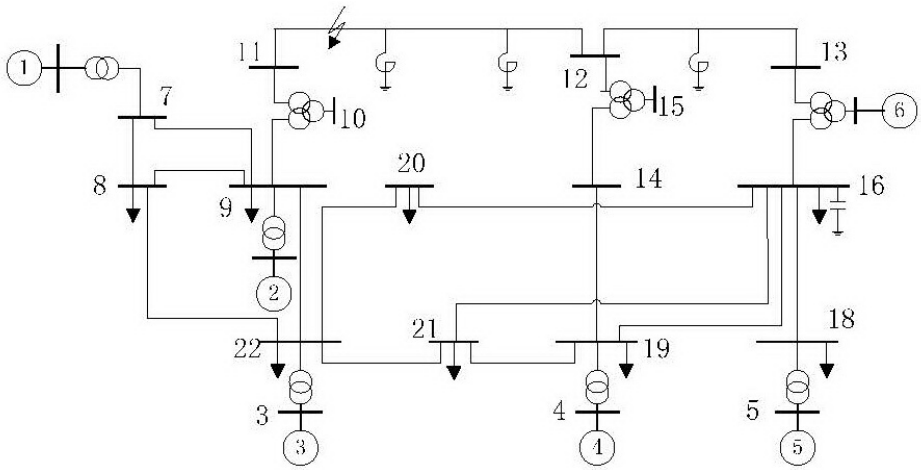

Figure 4. Voltage curve of key bus 11.

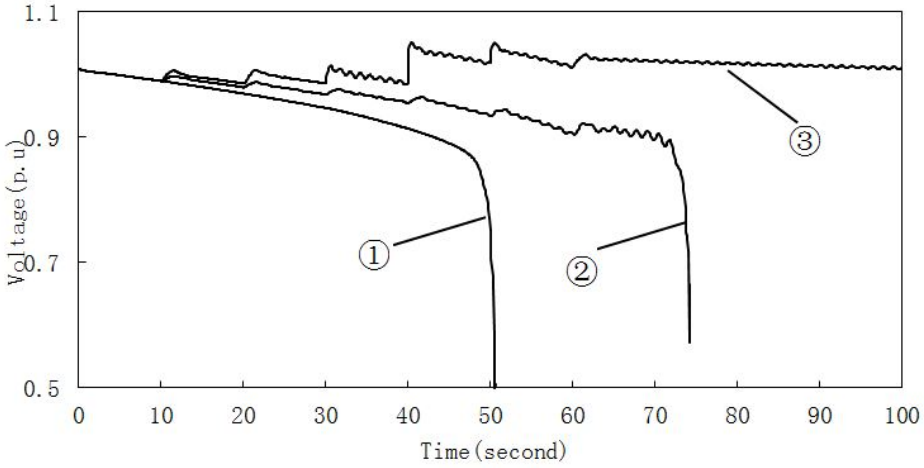

Figure 5. Voltage curve of key bus 16.

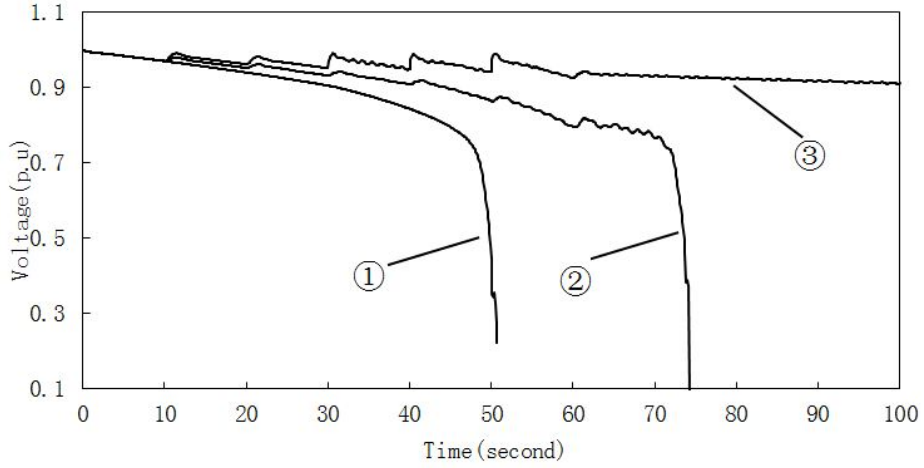

Figure 6. Voltage curve of generator 2.

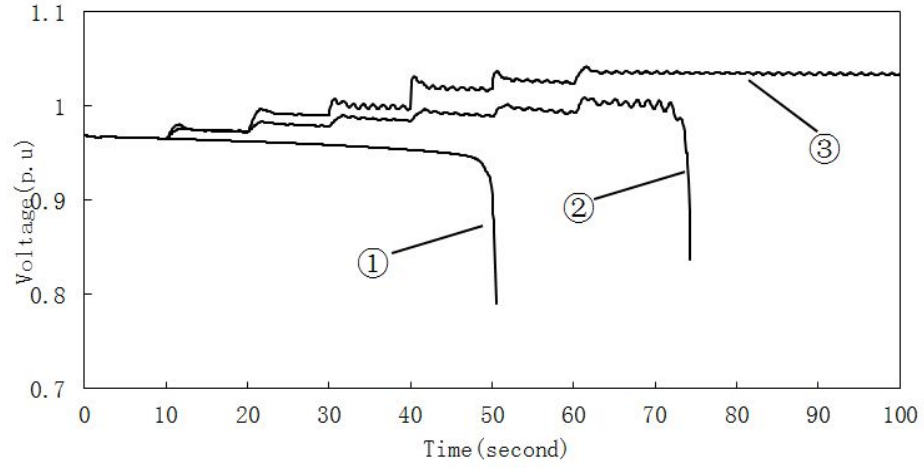

Figure 7. Active power curve of generator 2.

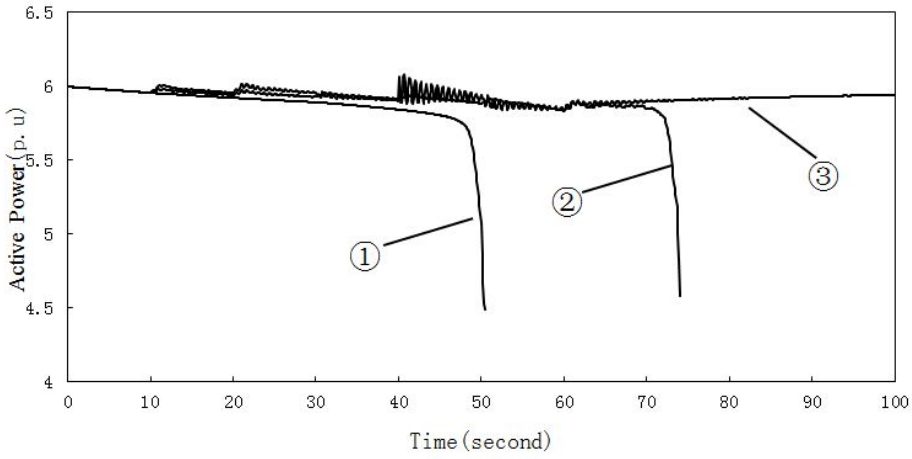

Figure 8. Reactive power curve of generator 2.

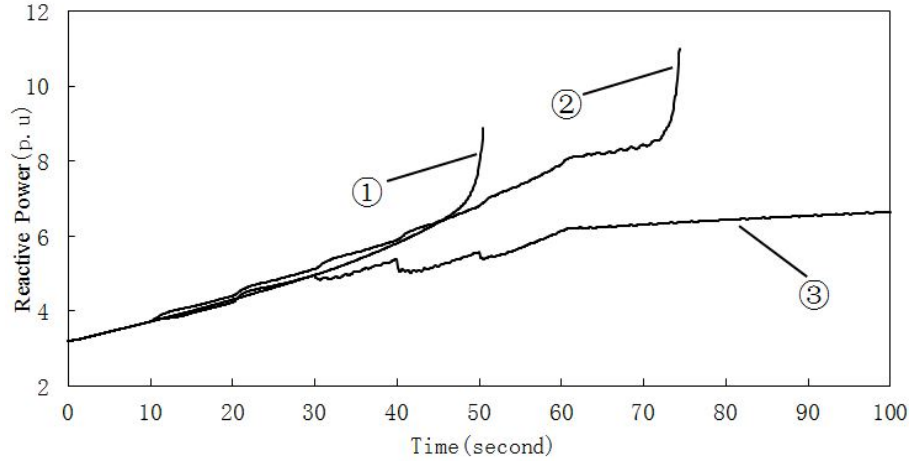

6.2. Simulation in NCPG's Power Grid

The Northeast China Power Grid is a 500 kV and 200 kV grid. It is located in the Hei Longjiang, Jin Lin and Liao Ning Provinces, also in the east part of Nei Menggu province.

The NCPG's 500 kV grid structure is shown as in Figure 9, where the parameters of the power system, generators and transformers are introduced also in reference [7]. A model of constant impedance (60%) combined with induction load motor (40%) is adopted. In the simulation, the reactive load in each load bus is evenly doubled from second 0 to second 60. Under such circumstances the three following programs are studied by comparison: ① traditional AVR control applied to all the generators; □ traditional secondary voltage control applied to all the generators; ③ hierarchical control applied to all the generators, with certain load-shedding and reactive power devices taken into consideration at the same time. The control interval is defined as 10 s. Liaoyang, Hanan and Hexin are selected as the pilot buses.

Figures 10–12 show the voltage curves of key buses Liaoyang, Hanan and Hexin in the three control programs mentioned, respectively. Figures 13–16 show the generator angle, voltage, output active power and reactive power curve of generator bus Yinmin. The above figures indicate that the system starts voltage collapse in about 50 s when traditional AVR control is applied. The situation is

improved when traditional secondary voltage control is applied, with the system starting voltage collapse in about 60 s. However, with the proposed dynamic hybrid automatic voltage control, the system is under effective control, with system security enabled and voltage collapse avoided.

Figure 9. NCPG 500 kV Grid structure.

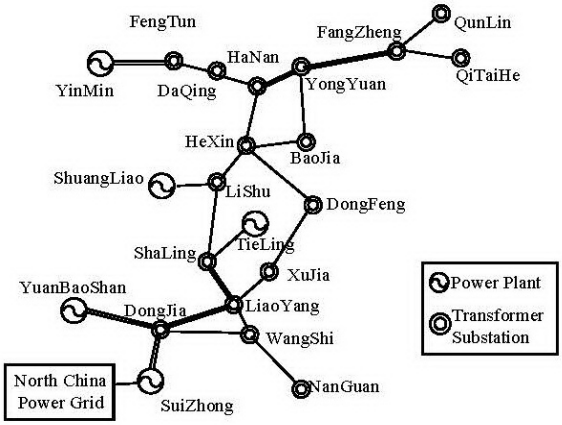

Figure 10. Voltage curve of key bus Liaoyang.

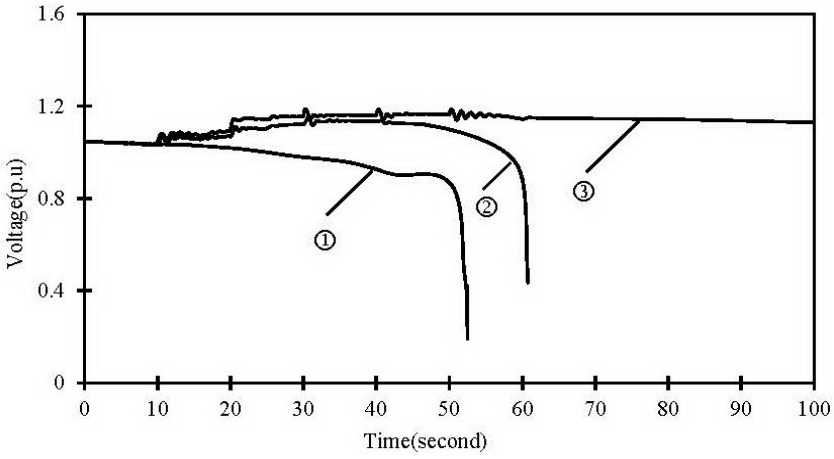

Figure 11. Voltage curve of key bus Hanan.

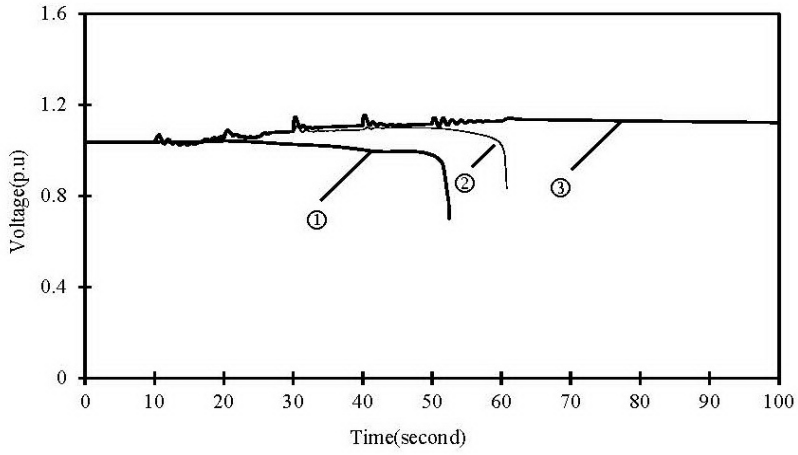

Figure 12. Voltage curve of key bus Hexin.

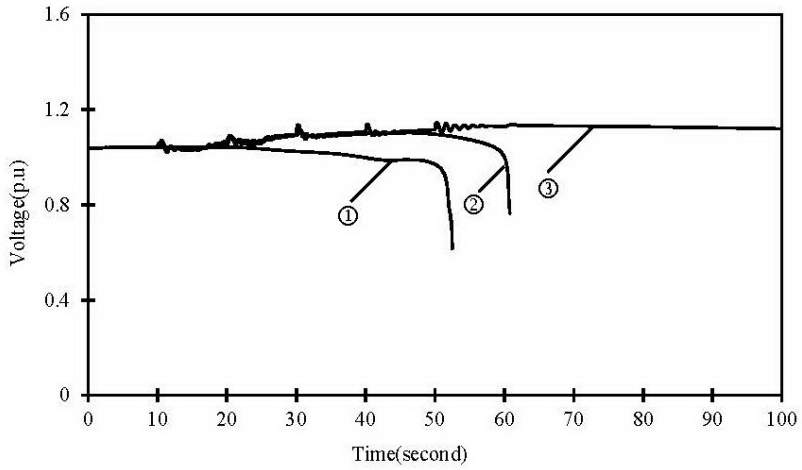

Figure 13. Generator Angle of key bus Yinmin.

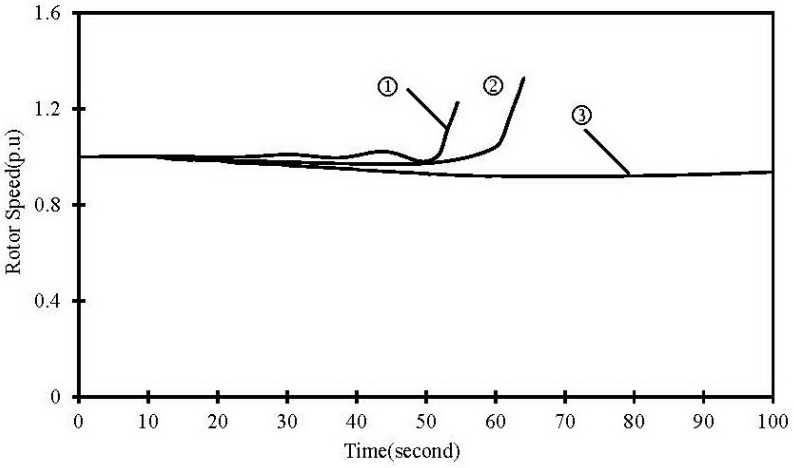

Figure 14. Voltage curve of bus Yimin.

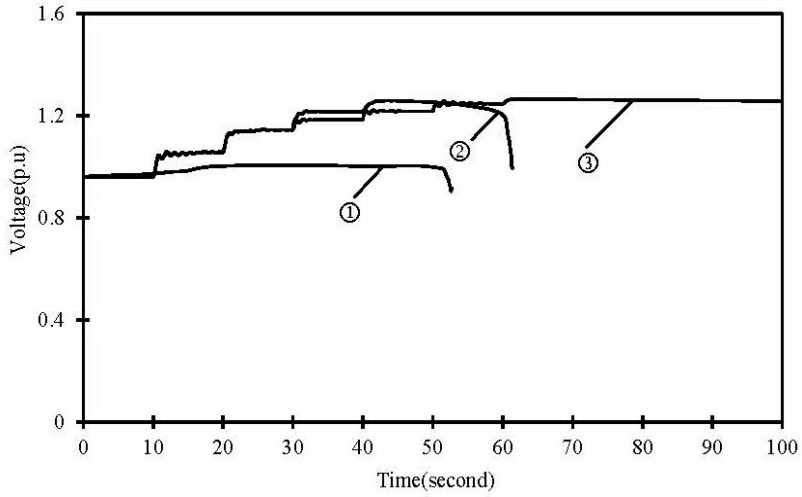

Figure 15. Output active power of bus Yimin.

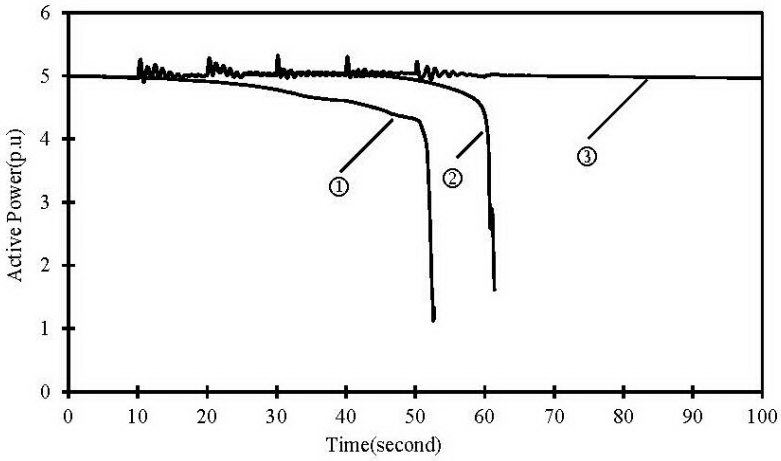

Figure 16. Output reactive power curve of bus Yimin**.**

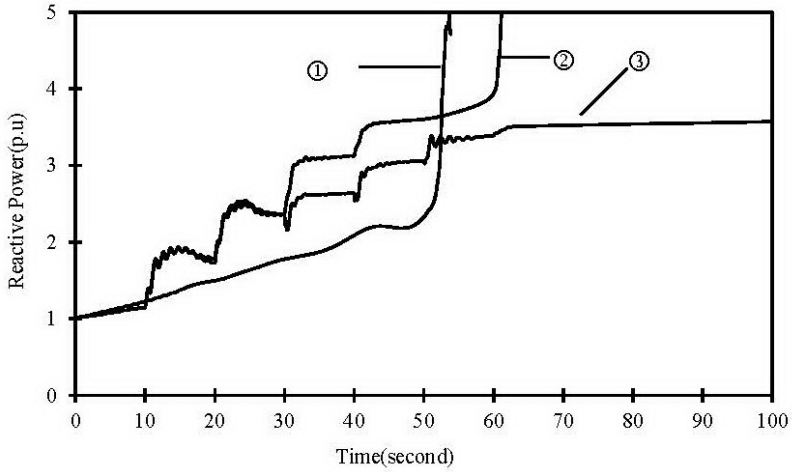

7. Conclusions

This paper focuses on dynamic voltage stability control. First of all, an HD-AVC system model is set up based on the hybrid system theory and methods. In such a system, the models of the Top Layer responsible for control and the Middle Layer responsible for management and operation are constructed in details. In the Top Layer, the power system's differential-algebraic-equations are linearized, and the eigen-matrix's minimum amplitude eigenvalue (MAE) is used to judge the power system's voltage security. In this way, discrete events are constructed to drive the control block. In the Middle Layer, driven by the discrete events, the control values of the control buses are calculated by applying the sensitivity method. Then the control strategies are made in the interface block. The control equipment in the Bottom Layer receives the control strategies and executes them, thus achieving closed-loop automatic voltage control. Computer simulation comparisons with secondary voltage control (SeVC) have proven the solution is effective in realizing a HD-AVC system.

Acknowledgment

This work was supported by China's National High Technology Research and Development Program (2011AA05A112), National Nature Science Foundation under Grant 51190101 and 50607011, Science and Technology Projects of the State Grid Corporation of China, also supported by the research projects of China's Hubei Electric Power Corporation and Liaoning Electric Power Company Limited.

Conflict of Interest

The authors declare no conflict of interest.

References

1. Taylor, G.W. *Power System Voltage Stability*; McGraw-Hill: New York, NY, USA, 1994; pp. 134–153.
2. Van Cutsm, T.; Vournas, C. *Voltage Stability of Electric Power Systems*; Kluwer Academic Publishers: Boston, MA, USA, 1998; pp. 47–71.
3. Stankovic, A.; Ilic, M. Dominic Maratukulam Recent results in secondary voltage control of power systems. *IEEE Trans. Power Syst.* **1991**, *6*, 94–10.
4. Sancha, J.L.; Fernandez, J.L.; Ortes, A.C.; Abarca, J.T. Secondary voltage control: Analysis, solutions and simulation results for the spanish transmission system. *IEEE Trnas. Power Syst.* **1996**, *11*, 630–638.
5. Ilic, M.D.; Liu, X.J.; Leung, G.; Athans, M.; Vialas, C.; Pruvot, P. Improved secondary and new tertiary voltage control. *IEEE Trans. Power Syst.* **1995**, *10*, 1851–1862.
6. Zheng, D.Z.; Zhao, Q.C. *Discrete Event Dynamic Systems*; Press of Tsinghua University: Beijing, China, 2002; pp. 24–66.
7. Wei, H. Studies on the Hybrid Automatic Voltage Control System. Ph.D. Thesis, Tsinghua University, Beijing, China, 2002.
8. Ni, Y.X.; Chen, S.S.; Zhang, B.L. *Theory and Analysis of Dynamic Power System*; Press of Tsinghua University: Beijing, China, 2002; pp. 231–242.
9. Zhang, B.M.; Chen, S.S. *Advance Electric Network Analysis*; Press of Tsinghua University: Beijing, China, 1996; pp. 45–123.
10. Yu, Y.X. Review on voltage stability studies. *Autom. Electr. Power Syst.* **1999**, *23*, 1–8.